FIRST TEST RUN FOR HIGH DENSITY MATERIAL IMAGING EXPERIMENT USING RELATIVISTIC ELECTRON BEAM AT THE ARGONNE WAKEFIELD ACCELERATOR

Y.R. Wang, Z.M. Zhang#, S.C. Cao, Q.T. Zhao, X.K. Shen, IMP, CAS, Lanzhou 730000, China
M. Conde, D.S. Doran, W. Gai, W. Liu, J.G. Power, C. Whiteford, E.E. Wisniewski
ANL, Argonne, IL 60439, USA
J.Q. Qiu, Euclid Techlabs, LLC, Solon, USA

Abstract

Argonne Wakefield Accelerator (AWA), has been commissioned and in operation since last year. It can provide beam of several bunches in a train of nanoseconds and 10s of nC with energy up to 70 MeV. In addition, the AWA can accommodate various beamlines for experiments. One of the proposed experiments is to use the AWA beam as a diagnostics for time resolved high density material, typically a target with high Z and time dependent, imaging experiments. When electron beam scatters after passing through the target, the angular and energy distribution of beam depend on the density and thickness of the target. A small aperture is used to collimate the scattered electron beam for off axis particles, and the target image will be detected by imaging screen. By measuring the scatted angle and energy at the imaging plate would yield information of the target. In this paper, we report on the AWA electron imaging (EI) system setup, which consist of a target, imaging optics and drift. The AWA EI beam line was installed on June, 2016 and the first test run was performed on August, 2016. This work will have implication on the high energy density physics and even future nuclear fusion studies. The details of AWA EI experiment setup, results, analysis and discussions are presented here.

INTRODUCTION

High energy density physics aims to study the properties of matter under extreme states of high temperature and high pressure. A new scheme based on high-energy electron beam as a probe was proposed for time-resolved imaging measurement of high energy density materials, especially for high energy density matter and inertial confinement fusion (ICF) [1, 2]. Comparing with proton and other x-ray diagnostics systems, electron imaging based on photo injector linear accelerator systems (LINAC) is expected to gain high spatial and temporal resolution at lower cost. Los Alamos National Lab developed the first high-energy electron radiography concept [3] with a 30 MeV electron beam achieving a resolution of 100 um. The first text run for high density material imaging experiment using relativistic electron beam at AWA was done. The imaging system was based on the AWA drive beamline with 50 MeV beam. The highest beam energy of AWA drive beam is 70 MeV, but for the electron imaging experiment, the energy of 50 MeV is chosen for stable running.

zzm@impcas.ac.cn

DESCRIPTION & OPTICS DESIGN OF AWA ELECTRON IMAGING SYSTEM SETUP

The first run for EI experiment in AWA was performed using drive beam. Figure 1 shows a schematic of the AWA drive beamline. The drive beam is generated by a photocathode RF gun running at 1.3 GHz. The drive gun is followed by 6 linac tanks (1.3 GHz) that bring the beam energy up to 70 MeV. The beam after 6 linac tanks is transported into dogleg which consists of two dipoles. For simplicity, the dogleg section is not designed for electron imaging experiment purposely. The dogleg is followed by AWA electron imaging experiment system which showed in Figure 2. It consists of two quadruples, target, one triplet, collimator and imaging plate.

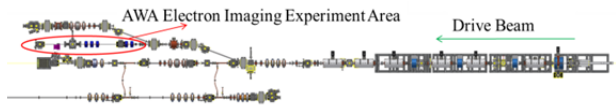

Figure 1: AWA drive beamline layout.

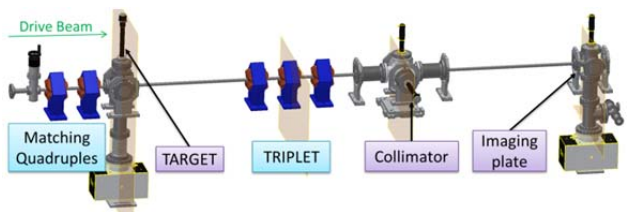

Figure 2: AWA electron imaging experiment system.

In AWA electron optical imaging system design, the beam energy of 50 MeV was chosen because of the power limitation of dogleg. The first two quadruples before target is used to matching the beam. The target crossing composed of a YAG screen, a bowtie shape mask with 10 mm long and 2.43 mm height segments, and a 200 um thick aluminium triangle part. The details of target cross are showed in figure 3.

The optical imaging system starts from target to imaging screen, which consists of one triplet and drift sections. The optical imaging system design is the key part in EI beamline, which was optimized by Transport code [4]. For electron imaging system, two conditions need to be

satisfied, similar to the requirements of proton radiography [5]. First, the lattice should provide a point-to-point focus from object (target) to image (imaging plate). That is to say, the position of the particle on the screen should only depend on the original position of the particle exiting the target, without being affected by the angle. Second, the lattice should form a Fourier plane, where particles are sorted only by angle. One collimator was put at Fourier plane to cut off electrons with angles larger than specific number. Desirable spatial resolution could be achieved by carefully designing of the beamline with Figure 4 shows the optical imaging system with magnification of 2.13X.

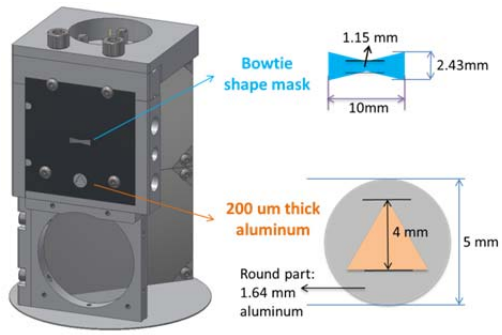

Figure 3: target layout.

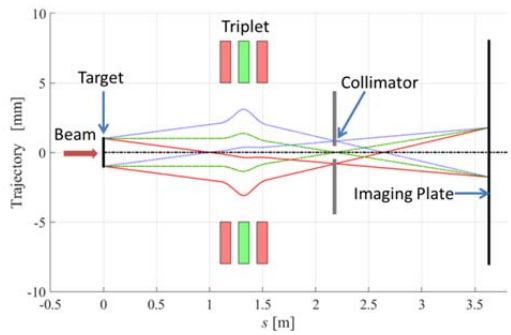

Figure 4: Layout of the optical imaging system.

An additional important design requirement is the resolution of the imaging system which is not specifically designed in the first test run imaging system. When high energy electrons traverse the target, they lose energy by bremsstrahlung. So the energy spread should be considered when study about the resolution of this system. The chromatic aberration coefficients define the final position errors for particles off the design momentum. The matrix elements in general are functions of the fractional momentum deviation $\delta = \Delta p / p$, so the final position of an off-momentum ray with initial coordinates (x, θ) is shown in formula (1).

$$x_s = R_{11}x + T_{116}x\delta + T_{116}x\theta \quad (1)$$

R is the first order transport matrix and T is the second order transport matrix.

The spatial resolution on the object plane is defined by formula (2), and M_x is the magnification in x plane which equals to R_{11}.

$$\Delta x = x_s/M_x - x = T_{116}x\delta + T_{116}x\theta/M_x \quad (2)$$

If a chromatically matched beam is introduced before the target,

$$\theta = -(T_{116}/T_{126}) \cdot x + \varphi$$

where φ represents the beam scattering angle after interacting with the target with residual incident angles.

After the calibration of the chromatically matched beam, the spatial resolution can be defined as formula (3), which depends on the chromatic length, scattering angle with residual incident angles and beam energy spread.

$$\Delta x = l_c \varphi \delta \quad (3)$$

where $l_c = T_{126}/M_x$ is the chromatic length.

In order to optimize the spatial resolution, one collimator with different apertures is placed on the Fourier plane which can cut off the beam with divergence angle bigger than σ ($\sigma < \varphi$). The collimated spatial resolution is defined by the formula (4),

$$\Delta x = l_c \sigma \delta \quad (4)$$

FIRST TEST RUN RESULTS AND ANALYSIS

The AWA electron imaging system composing one triplet and drift was designed and installed. For simplicity, the collimator with different apertures was taken from another beamline in AWA, Therefor, the thickness and the apertures are not optimised for this EI experiment. Also the collimator position was undetectable. The unwanted beam with energy spread around 5% was injected into the target, which influenced the final spatial resolution. Base on the EI system mentioned above, the first test run was performed. The quadruples before the target were used to acquire an approximately chromatically matched beam with the residual incident angles. The images were achieved with tuning the triplet fields and placing different apertures. The bowtie shape mask and aluminium triangle with 200 um thickness were imaged.

The images and RMS spatial resolution analysis of the bowtie shape mask are shown in figure 5. The RMS spatial resolutions with three different apertures are 0.362, 0.176 and 0.099 mm respectively. By comparing three different apertures in Figure5, it is clear that the images with aperture are significant improved. The aperture is important for the imaging system. Although the triplet field setting wasn't exactly the same in this three cases, we could roughly make a conclusion that smaller aperture is able to achieve better spatial resolution, which is consistent with the resolution formula (4) well. The beam energy spread was cancelled by apertures partially. The magnifications in X plane with three different apertures are 2.3, 2.4 and 2.4 times respectively, and the magnifications in Y plane with three different apertures are 2.3, 2.9 and 2.8 times respectively. Resulting from the unstable beam and undetected aperture positions, the magnetic strength of the triplet were adjusted accordingly. The different magnifications can be obtained with the different

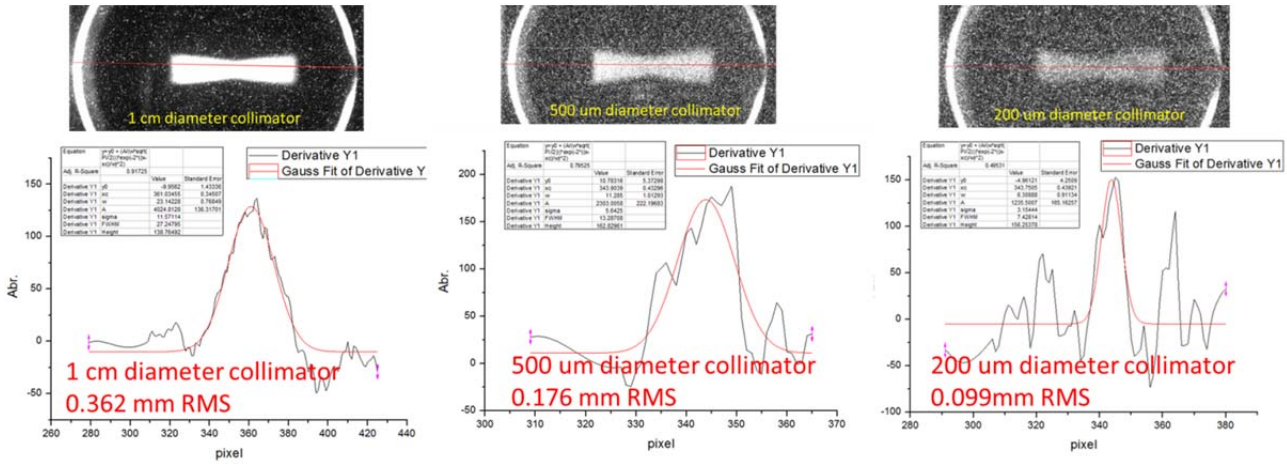

Figure 5: The bowtie shape mask images and the RMS spatial resolution analysis (guass fit) with three different apertures.

proper magnet strength. Typically, the higher magnification contributes to the spatial resolution by lowering the chromatic length.

The images and RMS spatial resolution analysis of the aluminium triangle with 200 um thickness is shown in figure 6. The RMS spatial resolution was obtained by calculating the average of the red mark region. The image was hardly to be observed by placing apertures, so the result only with no collimator was showed.

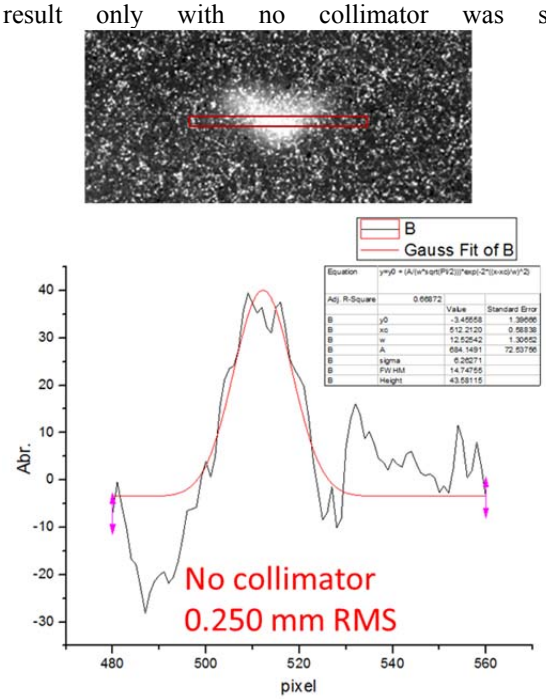

Figure 6: The triangle imaging and the RMS spatial resolution analysis (guass fit) with no aperture.

CONCLUSION

The first test run for electron imaging experiment in AWA was performed. The images of bowtie shape mask with different apertures showed the effect on spatial resolution by placing collimator in the Fourier plate. The magnification with 2.3 is consistent well with the designed value of 2.13 X. The experiment results are limited by several factors, including unwanted dogleg in beamline, undesigned collimator, and current diagnostics system.

The update of the AWA electron imaging system is under processing now, including the second order matrix optimization, new designed collimator and efficient diagnostics tools.

ACKNOWLEDGMENT

This work is supported by National Natural Science Foundation of China 11435015, 11505251 and China Scholarship Council (CSC NO.201500090009).

REFERENCES

[1] Y.T. Zhao, Z.M. Zhang, H.S. Xu, W.L. Zhan *et al.*, A high resolution spatial-Temporal imaging diagnostic for high energy density physics experiments, in: Proceedings of IPAC2014, Dresden, Germany, THOAB03, 2014, pp. 2819–2821.

[2] Wei Gai, Jiaqi Qiu, Chunguang Jing, Electron imaging system for ultrafast diagnostics of HEDP, in: Proceedings of the SPIE 9211, Target Diagnostics Physics and Engineering for Inertial Confinement Fusion III, 921104,2014.

[3] Frank Merrill, Frank Harmon, Alan Hunt, et al. Electron radiography, Nuclear Instruments and Methods in Physics Research B 261, 2007, 382–386.

[4] PSI Graphic Transport Framework by U. Rohrer based on a CERN-SLAC-FERMILAB version by K.L. Brown et al.

[5] C. T. Mottershead and J. D. Zumbro, in Particle Accelerator Conference, 1997. Proceedings of the 1997 IEEE,, pp. 1397.